Published in final edited form as:
Cornea. 2012 March ; 31(3): 273–279. doi:10.1097/ICO.0b013e3182254b42.

Changes of Chloride Channels in the Lacrimal Glands of a Rabbit Model of Sjögren's syndrome

Prachi Nandoskar[1], **Yanru Wang**[2], **Ruihua Wei**[3,4], **Ying Liu**[4,5], **Ping Zhao**[1,6], **Michael Lu**[1], **Jianyan Huang**[1], **Padmaja Thomas**[4], **Melvin D. Trousdale**[4], and **Chuanqing Ding**[1]

[1]Department of Cell and Neurobiology, University of Southern California, Keck School of Medicine, Los Angeles, CA 90089-9112

[2]Department of Physiology and Biophysics, University of Southern California, Keck School of Medicine, Los Angeles, CA 90089-9112

[3]Tianjin Medical University Eye Center

[4]Doheny Eye Institute

[5]Zhongshan Ophthalmic Center, Sun Yat-sen University

[6]Third Hospital of Hebei Medical University

Abstract

Purpose—To test the hypothesis that expression of Na^+-K^+-$2Cl^-$ co-transporter-1 (NKCC1), cystic fibrosis transmembrane conductance regulator (CFTR), and chloride channel 2 γ subunit (ClC2γ) in the lacrimal glands (LG) of rabbits with induced autoimmune dacryoadenitis (IAD) are changed.

Methods—LGs were obtained from adult female rabbits with IAD, and age-matched female control rabbits. LGs were processed for laser capture microdissection, real time RT-PCR, western blot, and immunofluorescence.

Results—In rabbits with IAD, mRNA abundances and protein expressions for NKCC1 and CFTR from whole LGs were significantly lower than in controls. mRNA abundances of NKCC1, CFTR, and ClC2γ from rabbits with IAD were significantly different from acini and ductal cells from controls. NKCC1 was localized to the basolateral membranes of all acinar and ductal cells, with weaker staining intensity in ductal cells, and the staining pattern from rabbits with IAD appeared similar to that from controls. CFTR was found as punctate aggregates in the apical cytoplasm of all acinar and ductal cells, with the intensity in ductal cells much stronger, and no significant difference between controls and rabbits with IAD. ClC2γ was also localized to the apical cytoplasm as punctate aggregates of all acinar cells, but not in ductal cells, and similar staining pattern was observed in rabbits with IAD to control rabbits.

All correspondence and reprint requests should be addressed to: Chuanqing Ding, MD, Ph.D., Dept. of Cell and Neurobiology, University of Southern California, Keck School of Medicine, 1333 San Pablo St., BMT 304, Los Angeles, CA 90089-9112, Tel: 323-442-3062, Fax: 323-442-3466, cding@usc.edu.

Commercial Relationship: None

Conclusions—Our data demonstrated significant changes of mRNA and protein expressions of NKCC1, CFTR, and ClC2γ in rabbits with IAD, suggesting that these changes may contribute to the altered lacrimal secretion, particularly Cl^- transport, in rabbits with IAD.

Keywords

lacrimal gland; chloride channels; dry eye; Sjögren's syndrome

1. Introduction

Sjögren's syndrome is an autoimmune disease, which causes functional impairment of the lacrimal and salivary glands, and is one of the most common causes of dry eye.[1] Although many theories have been proposed to understand the etiology of this debilitating disease, its causes are still largely unknown.[2]

Rabbits with induced autoimmune dacryoadenitis (IAD) mimic many of the ocular surface symptoms as well as lacrimal gland (LG) pathologic features characteristic of Sjögren's syndrome, and have been used extensively to study its pathophysiology.[3–5]

Like other exocrine secretions, lacrimal fluid is produced in two stages: 1) secretion of primary fluid in the acini and; 2) modification into the final fluid during transit through the duct system. Lacrimal fluid secretion is an osmotic process driven by the transepithelial secretion of electrolytes that is mediated by ion transporters and following water transport.[6–13]

Final lacrimal fluid has a much higher [Cl^-] and [K^+] than primary fluid, which resembles an isotonic ultrafiltrate of plasma,[14,15] suggesting ductal cells either secrete these two ions or reabsorb other ions to make [Cl^-] and [K^+] higher in the final fluid. Therefore Cl^- channels in the LG, particularly those in the duct system, are likely to play important roles.

Three ion transporters involved in Cl^- transport have been identified in the LG. Na^+-K^+-$2Cl^-$ co-transporter (NKCC), obligatorily couples fluxes of the three ions through plasma membranes. Two isoforms of NKCC have been identified so far: NKCC1 is expressed in many cell types, while NKCC2 is found only in kidney.[16] NKCC1 has been identified in the LGs of mouse,[10] rat,[11] rabbit,[13] and stimulation studies showed NKCC1 plays an important role in fluid secretion by the mouse exorbital LG.[10]

Cystic fibrosis transport regulator (CFTR), functions as a Cl^--selective channel that can mediate either influx or efflux, depending on the orientation of the Cl^- electrochemical potential gradient. CFTR has been found in the LGs of mouse,[17] rat,[11] rabbit,[13] and a mice knockout study suggested that CFTR plays a significant role in LG secretion, especially in the ducts.[17]

Chloride channel (ClC) is a superfamily of poorly understood ion channels consisting of approximately 13 members, which are responsible for transporting Cl^- across plasma membranes. ClC3 has been found in the rat LG,[11] and our recent report showed the presence of mRNA and protein of ClC2γ in the rabbit LG,[13] suggesting ClC may also play a role in Cl^- transport in LG secretion.

The aim of the present study is to investigate the changes of NKCC1, CFTR, and ClC2γ in rabbits with IAD, with the particular emphasis on the lacrimal duct system. We have compared findings of mRNAs of these three transporters from whole LGs, acinar cells, epithelial cells from various duct segments, and their protein expressions, from normal control rabbits and rabbits with IAD. Our results revealed significant changes of NKCC1,

CFTR, and ClC2γ in the LGs of rabbits with IAD and suggest that these changes may contribute to the reduced LG secretion in these animals.

2. Materials and Methods

2.1. Animals

Two groups of adult female New Zealand White rabbits (Irish Farms, Norco, CA) were used. One group consisted of three rabbits with IAD, auto-adoptively transferred by ex vivo-activated lymphocytes, while the other contained six age and sex matched normal controls. The procedures for IAD generation have been previously published.[3,4] Rabbits were narcotized with a mixture of ketamine (40 mg/ml) and xylazine (10 mg/ml) and given an overdose of Nembutal (80 mg/kg) for euthanasia. Inferior LGs were removed and embedded in OCT, frozen in liquid nitrogen, and stored at −80°C until use. This study conformed to the standards and procedures for the proper care and use of animals as described in the ARVO Statement for the Use of Animals in Ophthalmic Research.

2.2. Laser Capture Microdissection

Frozen sections were collected with PEN membrane-coated slides (Leica Microsystems), and stained with cresyl violet in RNase-free conditions with the LCM Staining Kit (Applied Biosystems, Foster City, CA). Areas of interest in tissue sections were then laser captured using a PixCell II LCM System (Arcturus Bioscience, Mountain View, CA). Approximately 100 cells were collected for each acinus and duct segment sample for isolation of total mRNA, and six replicates of each acinus and duct segment were collected from each animal.[13]

2.3. RNA extraction and reverse transcription

Total cellular RNA was isolated from RNALater-treated samples with RNeasy® midiKit plus on-column DNase digestion to reduce the possibility of DNA contamination (Qiagen, Valencia, CA). RNA quality and quantity was evaluated using a NanoDrop ND-1000 spectrophotometer (NanoDrop Technologies, Wilmington, DE). 5 μg of total RNA samples were then reverse-transcribed to cDNA only if the 260/280 ratio was above 1.9 (High Capacity cDNA Reverse Transcription Kit containing random primers and MultiScribe™ Reverse Transcriptase, Applied Biosystems) according to manufacturer's instructions.

2.4. Real time RT-PCR Analysis and Pre-amplification

The sequences of primers and probes used in this study were listed in our previous publication.[13] Sequences were selected using Primer Express™ software (Applied Biosystems) and synthesized by Applied Biosystems. All probes incorporated the 5′ reporter dye 6-carboxyfluorescein (FAM) and the 3′ quencher dye 6-carboxytetramethylrhodamine (TAMRA).

For LCM samples, pre-amplification was performed using TaqMan® PreAmp Master Mix Kit (Applied Biosystems). The pooled assay mix was prepared by combining up to 50 of 20× TaqMan® Gene Expression Assays into a single tube and using Nuclease-free water to dilute the pooled assays to a final concentration of 0.2×. The 50 μl of pre-amplification reaction included 25 μl of 2× TaqMan® PreAmp Master Mix, 12.5 μl of 0.2× pooled assay mix, and 12.5 μl of cDNA sample. The reactions were incubated in the DNA Engine® Thermal Cycler for 10 min at 95°C followed by 14 cycles at 95°C for 15 seconds and 4 minutes at 60°C and then held at 4°C. The pre-amplification product was then diluted 1:20 with 1× TE buffer and analyzed by TaqMan® real time RT-PCR.

For real time RT-PCR, amplification was carried out on the ABI PRISM® 7900HT Sequence Detection System (Applied Biosystems) using TaqMan® Gene Expression Master Mix (Applied Biosystems) containing the internal dye, ROX, as a passive reference. The PCR reaction volume was 10 µl. It contained 1×TaqMan® Gene Expression Master Mix, 300 nM forward and reverse primers, 250 nM probes, and 50 ng of cDNA template. The FAM signal was measured against the ROX signal to normalize for non-PCR-related fluorescence fluctuations. The cycle threshold (C_T) value represented the refraction cycle number at which a positive amplification reaction was measured and was set at 10× the standard deviation (SD) of the mean baseline emission calculated for PCR cycles 3−15. Each sample was measured in triplicate. The difference between the C_T values for each target mRNA and for the internal housekeeping gene, GAPDH, in each sample was used to calculate the abundance of target mRNA relative to the abundance of GAPDH mRNA in the same sample.

2.5. Immunofluorescence and Confocal Microscopy

Primary antibodies used were purchased from commercial vendors. The dilution for NKCC1 (goat polyclonal, N-16; Santa Cruz Biotechnology, Santa Cruz, CA) was 1:50; 1:250 for CFTR (mouse monoclonal; R&D Systems, Minneapolis, MN); and 1:100 for ClC2γ (mouse monoclonal; ABcam, Cambridge, MA). Secondary antibodies used were fluorescein isothiocyanate (FITC)-conjugated AffiniPure donkey anti-goat and anti-mouse IgG (Jackson ImmunoResearch Laboratories, West Grove, PA), at a dilution of 1:200. Rhodamine conjugated phalloidin, at the dilution of 1:200, was also used to stain F-actin to show the morphological profiles of LG.

The immunofluorescence technique has been described in detail previously.[13] Slides were observed with a confocal laser scanning microscope (Zeiss LSM 710). FITC-conjugated secondary antibodies were visualized by excitation at 488 nm using an argon laser. Images were analyzed with LSM image browser and PhotoShop (Adobe Systems, Mountain View, CA).

2.6. Western Blot

LGs were homogenized in isolation buffer (5% sorbitol, 0.5mM disodium EDTA, 0.2 mM phenylmethylsulfonyl fluoride, protease inhibitor cocktail, 5 mM histidine-imidazole buffer, pH 7.5), and centrifuged at 2000 g for 20 minutes. Supernatant was denatured in SDS-PAGE sample buffer for 20 minutes at 60 °C, resolved on a 4–20% gradient SDS-PAGE gel (Bio-Rad), and then transferred onto PVDM (Millipore Immobilon-P). To assess transporter proteins, a constant amount of proteins from each sample was analyzed. Membranes blots were probed with NKCC1 at the dilution of 1:200, CFTR at 1:1000, and ClC2γ at 1:250. All blots were incubated with Alexa 680-labeled donkey anti-goat or goat anti-mouse secondary antibody (Molecular Probes, Eugene, OR) and detected with an Odyssey Infrared Imaging System (Li-Cor, Lincoln, NE). Densitometry analysis of resulting gel was performed by the manufacturer's software.

2.7. Statistics

Student t-test was used to evaluate the significance of the differences and $P<0.05$ was considered as significant.

3. Results

3.1 Expression of mRNAs

NKCC1—The abundance of mRNAs for NKCC1 from whole LGs were significantly lower in animals with IAD ($P<0.05$), decreased from 2.543±0.161 to 0.882±0.082 (Fig. 1), a 65.3% decrease. Data from LCM samples indicated that mRNAs for NKCC1 were significantly more abundant in acini than in cells from any duct segments. mRNA levels of different duct segments were varied. NKCC1 mRNA level was significantly less abundant in acinar cells from rabbits with IAD than from control LGs.[13] Its abundance was significantly higher in interlobular and interlobar ducts in animals with IAD, as compared to those from control animals (Table 1).[13]

CFTR—CFTR mRNA abundance from whole LG was significantly lower in rabbits with IAD (0.005±0.001) as compared to controls (0.007±0.0008), a 22.9% decrease ($P<0.05$, Fig. 2). Data from LCM samples indicated that significantly higher abundance of CFTR mRNA was detected in all duct segments than in acini, and its abundance appeared to increase stepwise from intralobular to interlobar ducts. Compared to mRNA abundances form control animals, there was no significant differences in acini and all duct segments, except in intralobar duct, which was significantly lower ($P<0.05$) in rabbits with IAD (Table 1).[13]

ClC2γ—No significant difference of ClC2γ mRNA abundance from whole LG was detected between control and IAD animals ($P>0.05$, Fig. 3). LCM results showed that mRNA abundance of ClC2γ was the lowest in acini, interlobular and interlobar ducts, with the highest detected in intralobar duct. Compared to data from normal control rabbits, mRNA levels were significantly lower ($P<0.05$) in acini, interlobular and interlobar ducts (Table 1).[13]

3.2 Western Blot and Densitometry

by using immunoblotting of whole LG homogenates, we studied the expressions of NKCC1, CFTR, and ClC2γ, as shown in Fig. 4. Densitometry analysis showed that expressions of NKCC1 and CFTR from animals with IAD were 60% and 48% ($P<0.05$) less abundant than normal controls, while the level of ClC2γ from rabbits with IAD was 30% more than that of control animals ($P<0.05$).

3.3 Immunofluorescence

NKCC1—NKCC1-IR was observed in all acinar and ductal cells of both control and IAD animals. In acinar cells, staining was stronger on lateral membranes than on the basal membranes (Fig. 5). There was no staining of apical membranes of acinar and ductal cells in either control or IAD LGs. Ducts expressed weaker NKCC1-IR than acini, and no significant difference of distribution were observed between controls and rabbits with IAD.

CFTR—Extensive CFTR-IR was present as punctate aggregates within the apical cytoplasm of all acinar and ductal cells, while the intensity was much stronger in ductal cells (Fig. 6). CFTR-IR in control and IAD showed similar distribution patterns.

ClC2γ—Like CFTR-IR, ClC2γ-IR was also present as punctate aggregates within the apical cytoplasm of all acinar cells (Fig. 7). However, contrary to CFTR-IR, minimal ClC2γ-IR was detected in ductal cells. ClC2γ-IR distribution pattern in rabbits with IAD was similar to that of control animals.

4. Discussion

Our data demonstrated the significant variations of NKCC1, CFTR, and ClC2γ among acinar cells, and ductal cells from various duct segments. In normal control rabbits, acinar cells were rich in NKCC1 and ClC2γ, in support of their critical role in LG secretion.[13] Lacrimal fluid is first secreted as primary fluid by acinar cells and modified in the duct system. NKCC1 has been found to be expressed in the basolateral membranes of acinar and duct cells of the mouse exorbital LG, and in situ functional studies showed that it plays a significant role in fluid secretion.[10] In rat LG, NKCC1 has also been found in the basolateral membranes of duct cells, but not acinar cells.[11] The present data confirmed our previous report regarding the presence and distribution of NKCC1 in rabbit.[13]

While acinar cells represent 80% of all the epithelial cells in LG, ductal cells have been estimated to make up 15%.[18–20] Most of the previous studies of LG have focused on the acinar cells, with only a few have paid sufficient attention to the ducts. The expression of NKCC1 in the ducts, although with a lower abundance of mRNA and protein expression, certainly suggests active Na^+, K^+, and Cl^- in the ductal cells.

In contrast to the distribution pattern of NKCC1 in acinar and ductal cells, CFTR showed a predominant presence in the ducts at both mRNA and protein levels, strongly suggesting the ducts' active involvement in Cl^- transport. These results were in accordance with an elegant study from rat LG[11], which reported the detection of CFTR in the apical membranes of ductal cells. In fact, mouse mutant in CFTR gene has been shown having dilated acini that were presumably due to back-pressure caused by blocked ducts, and the mutant mice developed eye infections and were prone to persistent eye closure.[17] Patients with cystic fibrosis have the defect CFTR gene, and are reported to have dry eye. [21]

Contrary to the distribution patterns of both NKCC1 and CFTR, ClC2γ appeared to be evenly distributed among acinar and ductal cells, although its abundance varied significantly among duct segments. Ubels et al.[10] localized ClC3 in the apical membranes of rat lacrimal ductal cells, as well as in acinar cells, although their findings could not be verified by another study that only detected the mRNA and protein of ClC3 in rat submandibular gland, but not in LG.[22] However, other members of the ClC family have been found in salivary glands of mouse[23,24] and rat.[25]

We were unable to find any previous literature regarding the potential contributions of these three transporters to the reduced LG secretion in diseased state. However, studies in salivary glands, another exocrine glands that were very similar to LG anatomically and physiologically, showed that NKCC1[26,27], CFTR[28], and ClC2γ [22] play an important role in salivary secretion. Evans and colleagues[26] demonstrated that NKCC1 was localized to the basolateral membranes of acinar cells, but not duct cells, from parotid gland of wild-type mice. In NKCC1-deficient mice, however, a severe impairment of salivation was observed, and they concluded that NKCC1 was the major Cl^- uptake mechanism across the basolateral membrane of acinar cells and is critical for driving saliva secretion in vivo.

Apical Cl^- secretion across epithelial tissues provides the primary driving force for fluid secretion, and activation of apical Cl^- channels, in conjunction with Cl^- and Na^+ coupled entry mechanisms that would mediate secretion or absorption in apical and basolateral membranes, is the rate-limiting step for fluid secretion by most exocrine glands.[24,25,28] The altered transport of Cl^-, as suggested by the significant decrease of mRNAs for NKCC1 and CFTR from whole LGs, and significant changes of NKCC1 and CFTR proteins in acinar cells and epithelial cells from various duct segments from rabbits with IAD, strongly suggest that these changes may contribute to the reduced lacrimal secretion in rabbits with IAD, as documented before.[4,5] These data are also consistent with the notion that exocrine secretion

is dependent on NKCC1- and CFTR-mediated Cl^- transport.[10,24,26,28] However, the exact mechanisms of how these transporters mediate LG secretion in physiological and pathological conditions are unknown and certainly warrant further investigations.

ClC is a poorly understood group of Cl^- channels, although several isoforms have been found recently in LG.[11,13] The significant decrease of ClC2γ mRNA in interlobular and interlobar ducts from rabbits with IAD suggest decreased secretion or increased absorption of ClC2γ-mediated Cl^- transport in these two duct segments. However, considering CFTR is particularly rich in duct cells, ClC2γ-mediated Cl^- transport may not play a role as significant as that of CFTR. Functional studies, i.e., ex vivo perfusion studies by using dissected duct segments, may help to elucidate its role in LG secretion.

We acknowledge that changes of mRNA abundance and protein expression may not always correspond to each other, and does not necessarily correspond to their functional status; thus definite evidence must come from direct functional studies. It should also be noted that the mRNA abundances and protein expressions of NKCC1 in the rabbit LG was much higher than those of CFTR and ClC2γ, suggesting that NKCC1 plays a major role in Na^+, K^+, and Cl^- transport in the rabbit LG. In mouse exorbital LG, Walcott and colleagues[10] have elegantly demonstrated that NKCC1 is a significant player in fluid secretion. Moreover, both real time RT-PCR and immunofluorescence results from our study showed that NKCC1 was predominantly present in acinar cells, suggesting that acini are their major functional site.

The primary lacrimal fluid resembles an isotonic ultrafiltrate of plasma at all flow rates, while the final fluid has markedly different compositions depending on the flow rates, but generally with a much higher $[K^+]$ and $[Cl^-]$.[14,15] Non-mutually exclusive explanations for this phenomenon are: 1) duct cells secrete increased amounts of K^+ and Cl^-; and 2) duct cells reabsorb Na^+ and water to make the $[K^+]$ and $[Cl^-]$ in final fluid relative higher. The presence of the three Cl^- transporters in the duct cells strongly supports the first explanation. These data are in accordance with previous findings regarding lacrimal ducts' active role in LG fluid production.[6,7,11,13,29] We have found no published literature regarding the relative contribution the ducts make to the total volume of fluid secreted by the LG, although it has been estimated that the ducts may account for as much as 30% of the final volume in physiological conditions.[7]

Recent reports showed the beneficial effect of the ocular surface by the elevated $[K^+]$ in lacrimal fluid.[30,31] However, the benefit of having an elevated $[Cl^-]$ in the lacrimal fluid is unclear. The significant presence of NKCC1, CFTR, and ClC2γ in the duct system, particularly CFTR, which is predominantly localized to the ducts, certainly suggests that there is the need to have Cl^- secreted from the ducts, resulting in higher $[Cl^-]$ in final lacrimal fluid. Unfortunately, all the three transporters have not been studied in detail in the LG, let alone in the duct system. More studies into their roles are certainly needed.

We recognize that there are several other animal models that have been used widely for Sjögren's syndrome-related dry eye studies, especially murine strains with genetic mutations.[32–34] While studies using these models provide valuable information regarding the etiology of Sjögren's syndrome, the IAD model has also been demonstrated to be an excellent model and has been used extensively.[3–5] We believe studies using this rabbit model, one without genetic defect in contrast to the murine models, will also help us to understand the etiology of lacrimal dysfunction in Sjögren's syndrome.

In summary, our findings demonstrated that there were significant changes of mRNA and protein expressions of NKCC1, CFTR, and ClC2γ in rabbits with IAD. These changes occurred in both acinar cells and epithelial cells from various duct segments. These data strongly suggest that changes of NKCC1, CFTR, and ClC2γ may contribute to the altered

Cl^- transport in rabbits with IAD, although direct functional studies are needed to provide definite evidence. Data presented here also support previous findings that acini and ducts play different roles in LG secretion and both acinar and ductal epithelial cells can secrete lacrimal fluid.

Acknowledgments

This work was supported by NIH grants EY017731 (CD), EY012689 (MDT), EY03040 (Doheny Eye Institute Core), and DK048522 (Core Facilities of the USC Research Center for Liver Diseases). The authors thank Drs. Austin Mircheff and Joel Schechter for many helpful comments and discussions in experimental design and manuscript preparation; Leili Parsa, Tamako Nakamura, Michele MacVeigh, and Ernesto Barron for excellent technical support.

References

1. Pflugfelder S, Tseng S, Sanabria O, Kell H, Garcia C, Felix C, Feuer W, Reis B. Evaluation of subjective assessments and objective diagnostic tests for diagnosing tear-film disorders known to cause ocular irritation. Cornea. 1998; 17:38–56. [PubMed: 9436879]
2. Zoukhri D. Effect of inflammation on lacrimal gland function. Exp Eye Res. 2006; 82:885–898. [PubMed: 16309672]
3. Guo Z, Song D, Azzarolo A. Autologous lacrimal lymphoid mixed-cell reactions induce dacryoadenitis in rabbits. Exp Eye Res. 2000; 71:23–31. [PubMed: 10880273]
4. Zhu Z, Stevenson D, Schechter J. Lacrimal histopathology and ocular surface disease in a rabbit model of autoimmune dacryoadenitis. Cornea. 2003; 22:25–32. [PubMed: 12502944]
5. Thomas P, Zhu Z, Selvam S, Stevenson D, Mircheff AK, Schechter JE, Trousdale MD. Autoimmune dacryoadenitis and keratoconjunctivitis induced in rabbits by subcutaneous injection of autologous lymphocytes activated ex vivo against lacrimal antigens. J Autoimmun. 2008; 31:116–122. [PubMed: 18534818]
6. Dartt D, Moller M, Poulsen J. Lacrimal gland electrolyte and water secretion in the rabbit: localization and role of Na+/K+-activated ATPase. J Physiol. 1981; 321:557–569. [PubMed: 6461755]
7. Mircheff A. Lacrimal fluid and electrolyte secretion: a review. Curr Eye Res. 1989; 8:607–617. [PubMed: 2545410]
8. Herok GH, Millar TJ, Anderton PJ, Martin DK. Characterization of an inwardly rectifying potassium channel in the rabbit superior lacrimal gland. Invest Ophthalmol Vis Sci. 1998; 39:308–314. [PubMed: 9477987]
9. Herok GH, Millar TJ, Anderton PJ, Martin DK. Role of chloride channels in regulating the volume of acinar cells of the rabbit superior lacrimal gland. Invest Ophthalmol Vis Sci. 2008; 49:5517–5525. [PubMed: 19037000]
10. Walcott B, Birzgalis A, Moore L, Brink P. Fluid secretion and the Na^+, K^+, $2Cl^-$ cotransporter (NKCC1) in mouse exorbital lacrimal gland. Am J Physiol. 2005; 289:C860–C867.
11. Ubels J, Hoffman H, Srikanth S, Resau J, Webb C. Gene expression in rat lacrimal gland duct cells collected using laser capture microdissection: evidence for K^+ secretion by duct cells. Invest Ophthalmol Vis Sci. 2006; 47:1876–1885. [PubMed: 16638994]
12. Selvam S, Thomas P, Gukasyan H, Yu A, Stevenson D, Trousdale M, Mircheff AK, Schechter J, Smith R, Yiu S. Transepithelial bioelectrical properties of rabbit acinar cell monolayers on polyester membrane scaffolds. Am J Physiol Cell Physiol. 2007; 293:C1412–C1419. [PubMed: 17699637]
13. Ding C, Parsa L, Nandoskar P, Zhao P, Wu K, Wang Y. Duct system of the rabbit lacrimal gland: Structural characteristics and its role in lacrimal secretions. Invest Ophthalmol Vis Sci. 2010; 51:2960–2967. [PubMed: 20107177]
14. Alexander JH, van Lennep EW, Young JA. Water and electrolyte secretion by the exorbital lacrimal gland of the rat studied by micropuncture and catheterization techniques. Pflugers. Arch. 1972; 337:299–309. [PubMed: 4674879]

15. Rismondo V, Osgood TB, Leering P, Hattenhauer MG, Ubels JL, Edelhauser HF. Electrolyte composition of lacrimal gland fluid and tears of normal and vitamin A-deficient rabbits. CLAO J. 1989; 15:222–228. [PubMed: 2776293]

16. Russell JM. Sodium-potassium-chloride cotransport. Physiol Rev. 2000; 80:211–276. [PubMed: 10617769]

17. Ratcliff R, Evans MJ, Cuthbert AW, MacVinish LJ, Foster D, Anderson JR, Colledge WH. Production of a severe cystic fibrosis mutation in mice by gene targeting. Nat Genet. 1993; 4:35–41. [PubMed: 7685652]

18. Hisada M, Botelho SY. Membrane potentials of in situ lacrimal gland in the cat. Am J Physiol. 1968; 14:1262–1267. [PubMed: 5649481]

19. Herzog V, Sies H, Miller F. Exocytosis in secretory cells of rat lacrimal gland. Peroxidase release from lobules and isolated cells upon cholinergic stimulation. J Cell Biol. 1976; 70:692–706. [PubMed: 956271]

20. Parod RJ, Putney JW. An alpha-adrergic receptor mechanism controlling potassium permeability in the rat lacrimal gland acinar cell. J Physiol. 1978; 281:359–369. [PubMed: 212553]

21. Morkeberg JC, Edmund C, Prause JU, Lanng S, Koch C, Michaelsen KF. Ocular findings in cystic fibrosis patients receiving vitamin A supplementation. Graefes. Arch Clin Exp Ophthalmol. 1995; 233:709–713.

22. Majid A, Brown PD, Best L, Park K. Expression of volume-sensitive Cl(-) channels and ClC-3 in acinar cells isolated from the rat lacrimal gland and submandibular salivary gland. J Physiol. 2001; 534:409–421. [PubMed: 11454960]

23. de Santiago JA, Nehrke K, Arreola J. Quantitative analysis of the voltage-dependent gating of mouse parotid ClC-2 chloride channel. J Gen Physiol. 2005; 126:591–603. [PubMed: 16286506]

24. Romanenko VG, Nakamoto T, Catalan MA, Gonzalez-Begne M, Schwartz GJ, Jaramillo Y, Sepulveda FV, Figueroa CD, Melvin JE. Clcn2 encodes the hyperpolarization-activated chloride channel in the ducts of mouse salivary glands. Am J Physiol Gastrointest Liver Physiol. 2008; 295:G1058–G1067. [PubMed: 18801913]

25. Turner JT, Redman RS, Camden JM, Landon LA, Quissell DO. A rat parotid gland cell line, Par-C10, exhibits neurotransmitter-regulated transepithelial anion secretion. Am J Physiol. 1998; 275:C367–C374. [PubMed: 9688590]

26. Evans RL, Park K, Turner RJ, Watson GE, Nguyen HV, Dennett MR, Hand AR, Flagella M, Shull GE, Melvin JE. Severe impairment of salivation in Na+/K+/2Cl− cotransporter (NKCC1)-deficient mice. J Biol Chem. 2000; 275:26720–26726. [PubMed: 10831596]

27. Wellner RB, Redman RS, Swaim WD, Baum BJ. Further evidence for AQP8 expression in the myoepithelium of rat submandibular and parotid glands. Pflugers Arch. 2006; 451:642–645. [PubMed: 16311720]

28. Catalan MA, Nakamoto T, Gonzalez-Begne M, Camden JM, Wall SM, Clarke LL, Melvin JE. CFTR and ENaC ion channels mediate NaCl absorption in the mouse submandibular gland. J Physiol. 2010; 588:713–724. [PubMed: 20026617]

29. Tóth-Molnár E, Venglovecz V, Ozsvari B, Rakonczay Z Jr, Varro A, Papp J, Toth A, Lonovics J, Takacs T, Ignath I, Ivanyi B, Hegyi P. New experimental method to study acid/base transporters and their regulation in lacrimal gland ductal epithelia. Invest Ophthalmol Vis Sci. 2007; 48:3746–3755. [PubMed: 17652747]

30. Singleton KR, Will DS, Schotanus MP, Haarsma LD, Koetje LR, Bardolph SL, Ubels JL. Elevated extracellular K+ inhibits apoptosis of corneal epithelial cells exposed to UV-B radiation. Exp Eye Res. 2009; 89:140–151. [PubMed: 19289117]

31. Ubels JL, Schotanus MP, Bardolph SL, Haarsma LD, Koetje LR, Louters JR. Inhibition of UV-B induced apoptosis in corneal epithelial cells by potassium channel modulators. Exp Eye Res. 2010; 90:216–222. [PubMed: 19874821]

32. Zoukhri D, Hodges RR, Dartt DA. Lacrimal gland innervation is not altered with the onset and progression of disease in a murine model of Sjogren's syndrome. Clin Immunol Immunopathol. 1998; 89:126–133. [PubMed: 9787114]

33. Walcott B, Matthews G, Brink P. Differences in stimulus induced calcium increases in lacrimal gland acinar cells from normal and NZB/NZW F1 female mice. Curr Eye Res. 2002; 25:253–260. [PubMed: 12658559]

34. Ding C, MacVeigh M, Pidgeon M, da Costa SR, Wu K, Hamm-Alvarez SF, Schechter JE. Unique ultrastructure of exorbital lacrimal glands in male NOD and BALB/c mice. Curr Eye Res. 2006; 31:13–22. [PubMed: 16421015]

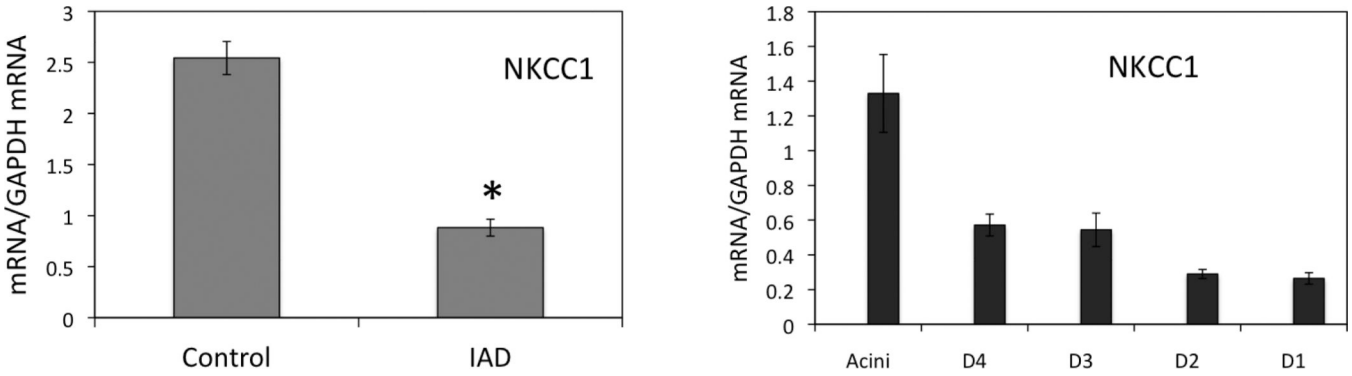

Fig. 1.

Real-time RT-PCR of NKCC1. mRNA abundance of NKCC1 from whole LG (left panel) of rabbits with IAD was significantly lower ($P<0.05$, indicated by *, same to all the following figures) than that of control rabbits, a 65.3% decrease. For LCM samples from rabbits with IAD (right panel), mRNA level was the highest in acini, and its abundance appeared to decreases as the ducts become bigger, with the lowest found in interlobar duct. D4: intralobular duct. D3: interlobular duct. D2: intralobar duct. D1: interlobar duct. Data were presented as mean±SEM.

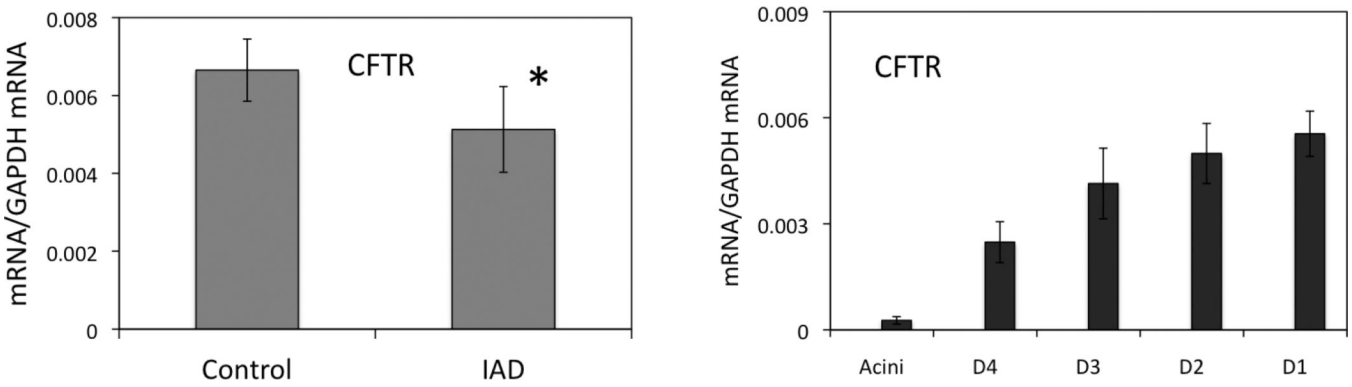

Fig. 2.

Real time RT-PCR of CFTR. CFTR mRNA level from whole LGs (left panel) of rabbits with IAD was significantly lower than control animals ($P<0.05$). For LCM samples from rabbits with IAD (right panel), mRNA was the least abundant in acini, while its abundance increase as the ducts become bigger, with the highest being in interlobar duct. D4: intralobular duct. D3: interlobular duct. D2: intralobar duct. D1: interlobar duct. Data were presented as mean±SEM.

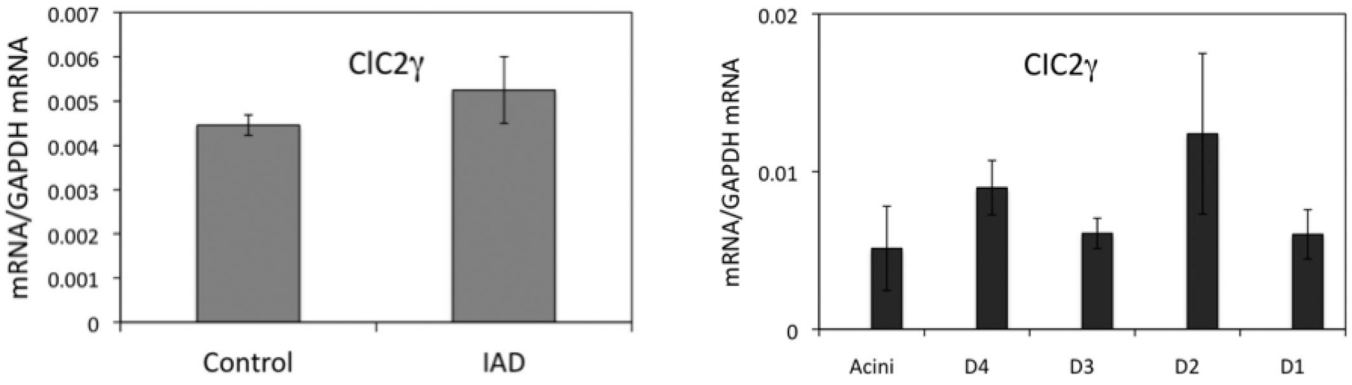

Fig. 3.

Real time RT-PCR of ClC2γ. ClC2γ mRNA level from whole LG (left panel) of rabbits with IAD was similar to that in controls ($P>0.05$). For LCM samples from rabbits with IAD (right panel), mRNA abundances were lowest in acini, interlobular and interlobar ducts, with the highest found in intralobar duct. D4: intralobular duct. D3: interlobular duct. D2: intralobar duct. D1: interlobar duct. Data were presented as mean±SEM.

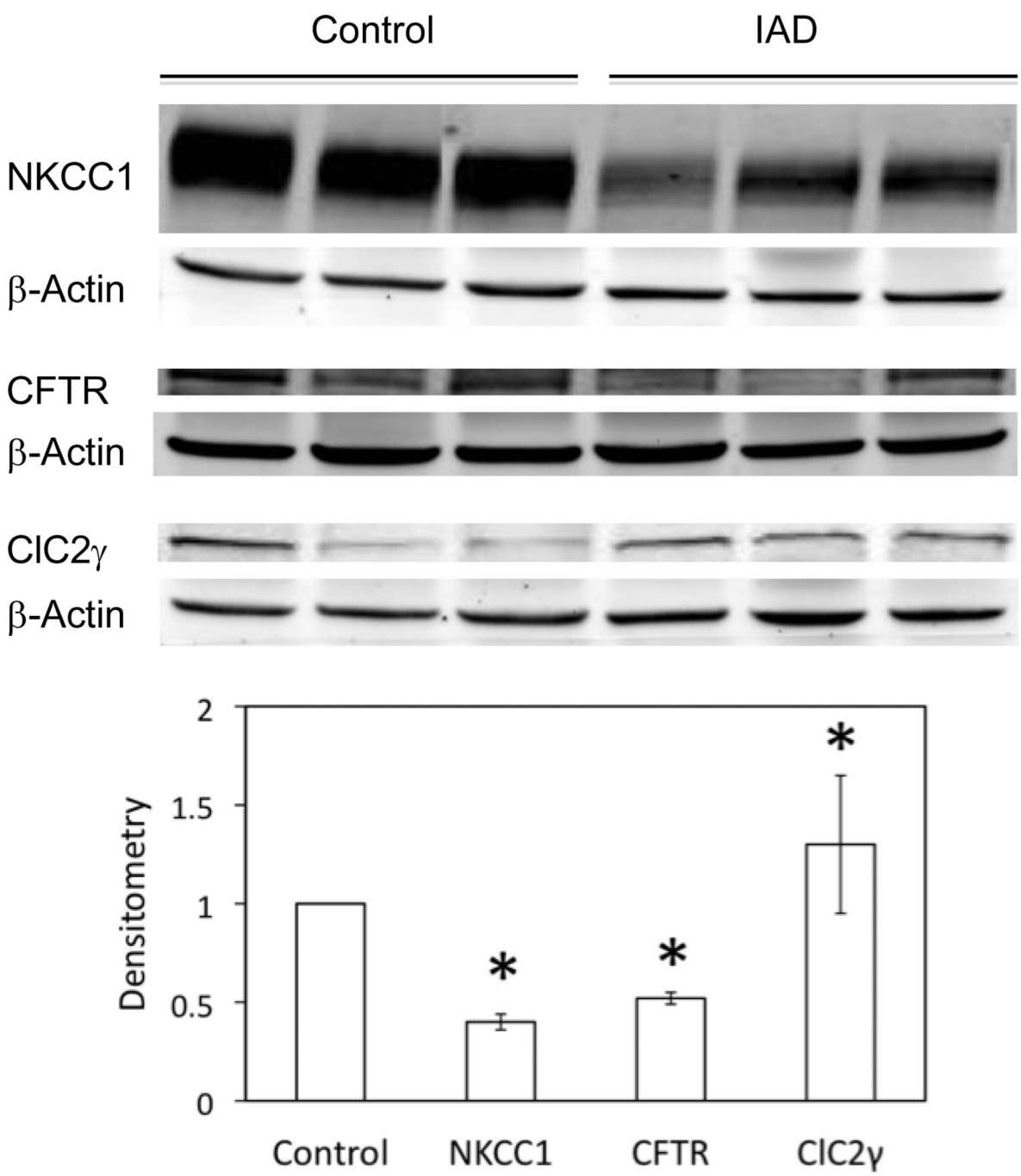

Fig. 4.

Western blots of NKCC1, CFTR, and ClC2γ from whole LG homogenates of both normal rabbits and rabbits with IAD. NKCC1 and CFTR were significantly decreased ($P<0.05$, indicated by *) in LGs from rabbits with IAD, while ClC2γ was significantly increased ($P<0.05$). Each well was loaded with 40 μg of protein. β-Actin was used as loading controls. N=3 each from three different animals.

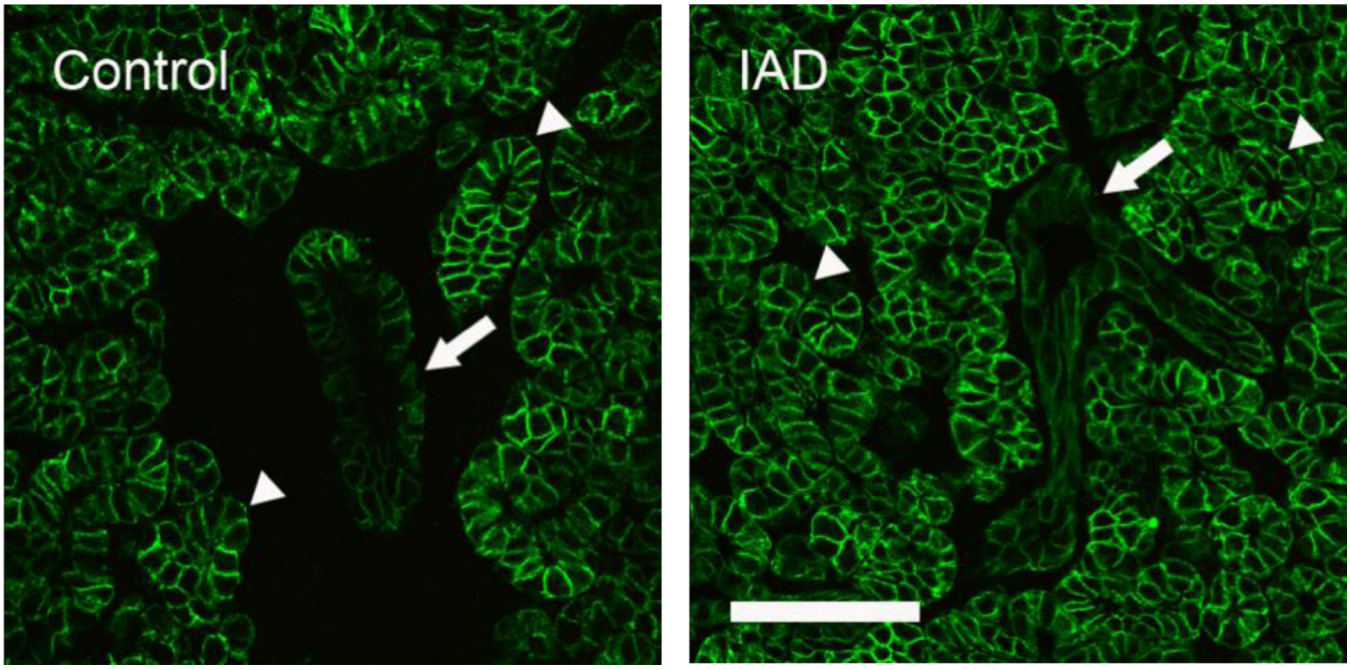

Fig. 5.

Immunofluorescence of NKCC1-IR. **Control:** NKCC1-IR was present at basolateral membranes of all acinar (arrowheads) and ductal cells (arrow), but the intensity was lower in ductal cells. **IAD:** NKCC1-IR in the acinar and ductal cells from IAD rabbits exhibited similar distribution pattern to that of control animals, with the staining intensity in ducts (arrow) was also much lower. Scale bar=50 μm.

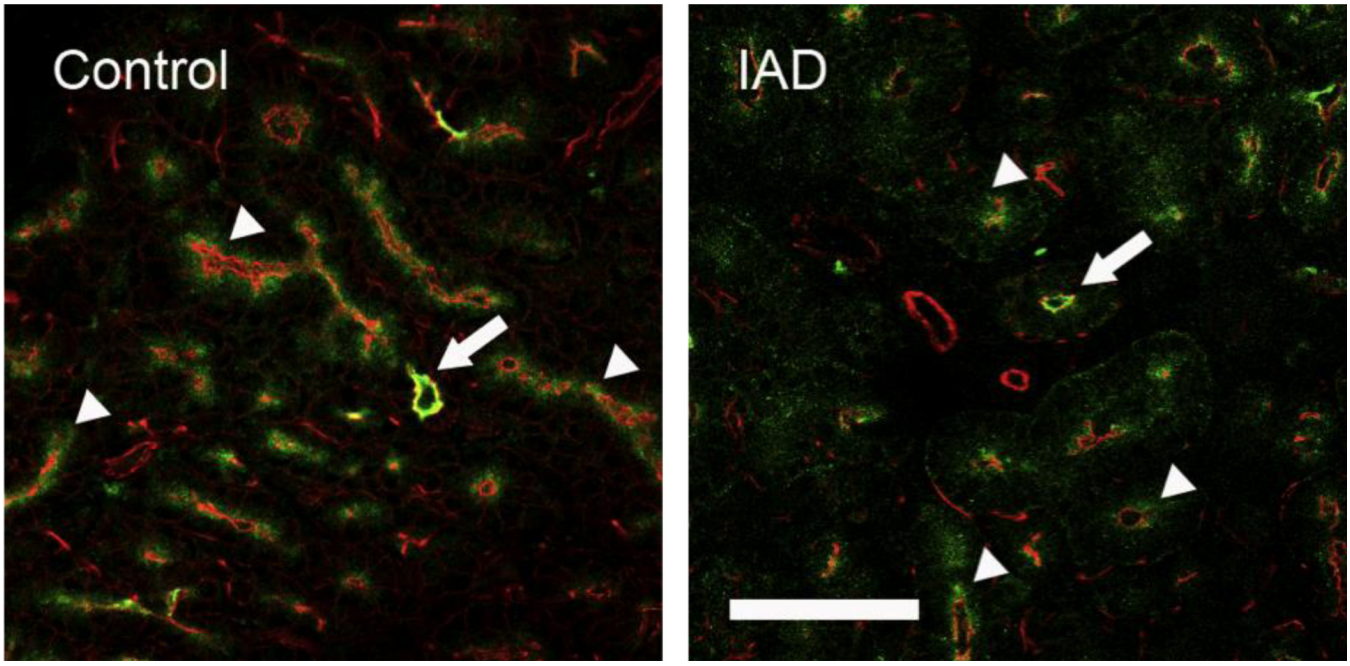

Fig. 6.

Immunofluorescence of CFTR-IR. **Control:** CFTR-IR (green) was present as punctuate aggregates within the apical cytoplasm of all acinar (arrowheads) and ductal cells (arrow), but the intensity in ductal cells was significantly higher. Rhodamine conjugated phalloidin, which stains F-actin, was used to outline the morphological profile (red). **IAD:** the distribution pattern of CFTR-IR in LGs from rabbits with IAD, both acinar (arrowheads) and ductal cells (arrow), was similar to those from control animals. Scale bar=50 μm.

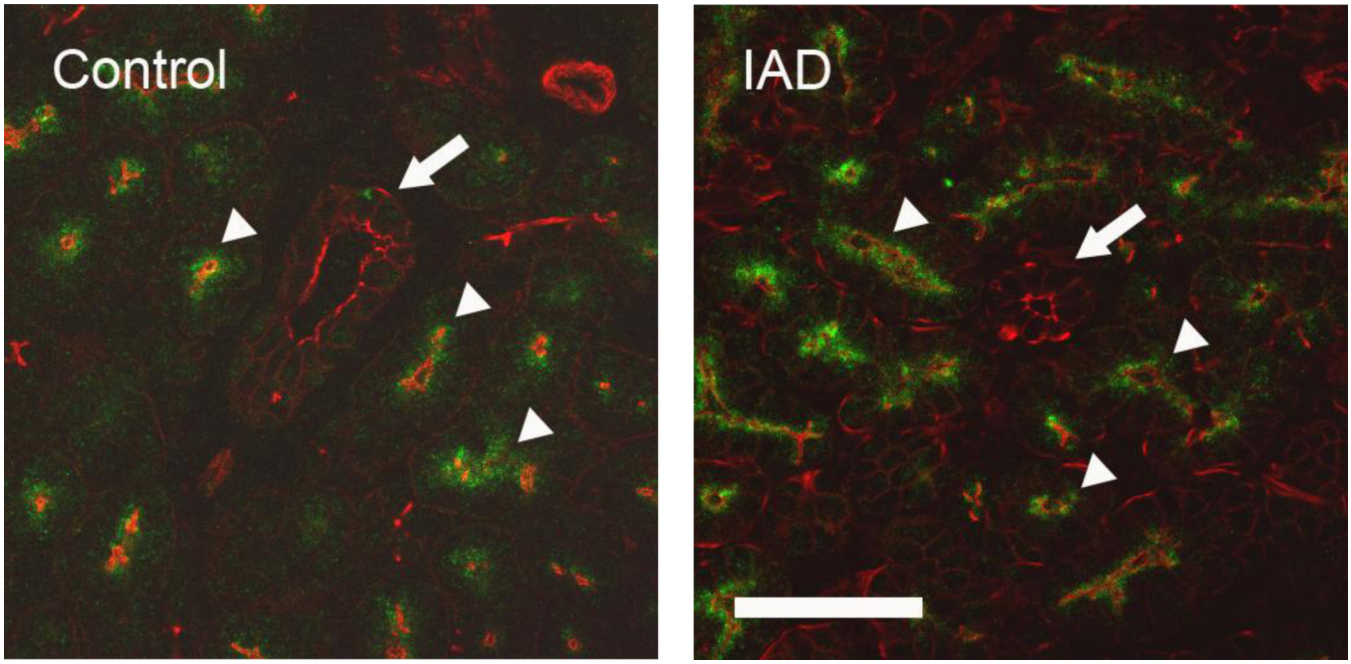

Fig. 7.

Immunofluorescence of ClC2γ-IR. **Control:** Like CFTR, ClC2γ-IR (green) was also found in the apical cytoplasm as punctate aggregates (arrowheads). Contrary to CFTR-IR, minimal ClC2γ-IR was seen in duct cells (arrow). Rhodamine conjugated phalloidin was used to outline the morphological profile (red). **IAD:** ClC2γ-IR was stained in a similar pattern as in control animals, both acinar (arrowheads) and ductal cells (arrow). Scale bar=50 μm.

Table 1

mRNA Changes of Epithelial Cells from Rabbits with IAD as Compared to Controls

	Acini	D4	D3	D2	D1
NKCC1	↓	–	↑	–	↑
CFTR	–	–	–	↓	–
ClC2γ	↓	–	↓	–	↓

Note: ↓: significant decrease; ↑: significant increase; –: no significant difference.